Kinetics of the Esterification of Acetic Acid with 2-Propanol: Impact of Different Acidic Cation Exchange Resins on Reaction Mechanism

SAMI H. ALI, SABIHA Q. MERCHANT

Chemical Engineering Department, Kuwait University, P. O. Box 5969, Safat 13060, Kuwait

ABSTRACT: The kinetics of the esterification of acetic acid with the secondary alcohol, 2-propanol, catalyzed by the cation exchange resins, Dowex 50Wx8-400, Amberlite IR-120, and Amberlyst 15 has been studied at temperatures of 303, 323, and 343 K; acid to alcohol molar ratios of 0.5, 1, and 2; and catalyst loadings of 20, 40, and 60 g/L. The equilibrium constant was experimentally determined, and the reaction was found to be mildly exothermic. External and internal diffusion limitations were absent under the implemented experimental conditions. Systems catalyzed by gel-type resins (Dowex 50Wx8-400 and Amberlite IR-120) exhibit some similarities in their reaction kinetics. Increase in reaction temperature, acid to alcohol ratio, and catalyst loading is found to enhance reaction kinetics for the three catalysts. The pseudohomogeneous (PH), Eley Rideal (ER), Langmuir Hinshelwood (LH), modified Langmuir Hinshelwood (ML), and Pöpken (PP) models were found to predict reaction kinetics with mean relative errors of less than 5.4%. However, the ML model was found to be better for predicting reaction kinetics in the systems catalyzed by gel-type resins, while the PP model was better for the system catalyzed by the macroreticular catalyst, Amberlyst 15. The E_{act} for the forward

reaction is found to be 57.0, 59.0, and 64.0 kJ/mole for the systems catalyzed by Dowex 50Wx8-400, Amberlite IR-120, and Amberlyst 15, respectively. For these three catalysts, the adsorption equilibrium constants of the components present in the system increase in the same order as do the solubility parameters of the component. Nonideality in the system is successfully accounted for by the UNIFAC model. © 2006 Wiley Periodicals, Inc. Int J Chem Kinet 38: 593–612, 2006

INTRODUCTION

Esters like 2-propyl acetate are desirable products having a variety of uses [1,2], and the esterification reaction is the most viable route [3,4] for producing these value-added products. Catalytic esterification along with distillation [5] or in conjunction with a simulated moving bed reactor [6] can also be used in the treatment of waste streams containing the acid or alcohol. Amongst the wide variety of catalysts available, cation exchange resins are gaining popularity as they are ecofriendly, noncorrosive, and have good thermal stability [7–11]. Studies on cation exchange resin catalyzed esterification of acids with primary alcohols have been extensively covered by earlier workers [5,6,12–26]. However, the same is not true for cation exchange catalyzed esterification of acids with secondary alcohols; very few of such studies can be found in open literature [14,15,22,25,27]. Moreover, a comparison of the kinetics of esterification of primary and secondary alcohols with acids, as done by earlier workers [14,22,25], clearly indicates significant differences in the respective reaction kinetics. This is one of the main reasons for studying the esterification kinetics of the secondary alcohol, 2-propanol with acetic acid.

Moreover, with the exception of very few published papers [14,24], literature was found to be lacking in detailed studies on the kinetics of esterification reactions with Amberlite IR-120, a common gel-type catalyst which could hold good potential under the right conditions. Some authors have carried out just a few preliminary experiments on the esterification kinetics of Amberlite IR-120 to compare its activity with that of other catalysts [5,23,27]. Under the arbitrarily chosen reaction conditions employed by these workers, Amberlite IR-120 was not found to exhibit the best kinetic activity; hence, detailed kinetic studies with this catalyst were not performed. Furthermore, both El Naomany et al. [14] and El Ewady et al. [24] interpret the kinetics on this catalyst with simple power law type of equations. No attempts have been made to predict the kinetics using the more advanced models (like the Eley Rideal or Langmuir Hinshelwood models) which take into account the selective adsorption of the components present.

Furthermore, industries routinely optimize reaction conditions/parameters, such as temperature, initial acid to alcohol ratio, and catalyst loading, to achieve target conversions. The nature and type of catalyst used, in conjunction with these conventional reaction parameters, will also strongly influence the time required to reach the target conversion. For this purpose, there is a need to compare the performance of common and easily available catalysts over a range of reaction conditions. However, the studies comparing catalyst activities available in open literature [5,12,19,23,26,27] are limited to a few arbitrarily chosen runs. Hence, there is a need for studies where the performance of the chosen catalysts is systematically studied over a range of temperature, acid to alcohol loading, and catalyst concentrations.

These factors are the main impetus for the current study on the esterification of acetic acid with the simplest possible secondary alcohol, namely 2-propanol, using three different cation exchange resins, namely Dowex 50Wx8-400, Amberlite IR-120, and Amberlyst 15. The aim of this work is to

(i) systematically study the effect of temperature, acid to alcohol molar ratio, and catalyst loading on the esterification of acetic acid with 2-propanol, over three cation exchange catalysts, namely, Dowex 50Wx8, Amberlite IR-120, and Amberlyst 15;

(ii) correlate the kinetic data with a number of accepted mathematical models and compare the performance of the tried models;

(iii) compare the kinetic as well as the adsorption terms of the three different catalysts.

THEORY

Esterification reactions are equilibrium-limited chemical reactions. Acetic acid reacts with 2-propanol to give the corresponding ester, 2-propyl acetate. The overall reaction is as follows:

$$CH_3COOH + (CH_3)_2CHOH$$
$$\leftrightarrow CH_3COOCH(CH_3)_2 + H_2O \qquad (1)$$
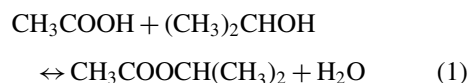
Reversible second-order kinetics which is usually applied for homogeneously catalyzed esterification reactions [28–30] has been used by some authors [13,31–33] for reactions catalyzed by heterogeneous catalysts like ion-exchange resins.

The sulfonic acid groups present on the solid catalysts being studied initiate the esterification reaction mechanism [34,35] by donating a proton to the carboxylic acid molecule. After the proton transfer, the carboxylic acid is accessible for a nucleophilic attack by the hydroxyl group from the alcohol, and the reaction continues with water elimination. In the final stage, the catalyst is recovered. The proton-donating step is usually assumed to be rapid, while the nucleophilic substitution is slow. The overall rate equation for the reaction can be expressed by

$$r_i = n \frac{\mathrm{d}\, x_i}{\upsilon_i\, \mathrm{d}t} = M_{\mathrm{cat}} k_f \left(a_{aa} a_{ipa} - \frac{1}{K} a_{\mathrm{ester}} a_w \right) \quad (2)$$

where M_{cat} is the catalyst mass, n is the total number of moles, υ_i is the stoichiometric coefficient of the ith component, a_i is the activity of the ith component in the bulk liquid phase ($a_i = x_i \gamma_i$), x_i is mole fraction of the ith component, and γ_i is the activity coefficient of the ith component. k_f is the forward reaction rate constant, and K is the equilibrium constant.

Pöpken et al. [20] tried to predict the reaction kinetics of the esterification reaction using both concentrations as well as activities of the components present. He found the use of the latter quantity leads to a more consistent and accurate kinetic description. The activity coefficient of the ith component according to the Universal Functional group Contribution (UNIFAC) model [36] can be calculated from the equation

$$\ln \gamma_i = \ln \gamma_i^{\mathrm{comb}} + \ln \gamma_i^{\mathrm{res}} \quad (3)$$

The residual part of the activity coefficient is given by

$$\ln \gamma_i^{\mathrm{res}} = \sum_k \nu_k^{(i)} \left(\ln \Gamma_k - \ln \Gamma_k^{(i)} \right) \quad (4)$$

And the combinatorial part [37] has the following form:

$$\ln \gamma_i^{\mathrm{comb}} = \ln \frac{\varphi_i}{x_i} + 1 - \frac{\varphi_i}{x_i} + SG \quad (5)$$

where SG, the Staverman–Guggenheim correction term, is the term generally added to models to account for the effect of differences in shapes of molecules.

However, the pseudohomogeneous (PH) model, as expressed by Eq. (2), does not take into account the different sorption effects of the involved species [38]. This drawback is generally overcome by the use of models which account for the differences in the affinities of the components present in the system (2-propanol, acetic acid, 2-propyl acetate, and water) for the ion-exhange resins being used (Dowex 50Wx8-400, Amberlite IR-120, and Amberlyst 15). Sorption effects are accounted for by incorporating adsorptions terms in the models discussed below.

The ER model: Depending on which of the two reactants is adsorbed, for a single site surface reaction rate controlling step, the reaction between an adsorbed and a nonadsorbed reactant molecule resulting in an adsorbed water molecule on the catalyst surface and a nonadsorbed ester molecule can be represented by the Eley Rideal model:

$$\begin{aligned} r_i &= n \frac{\mathrm{d}x_i}{\upsilon_i\, \mathrm{d}t} \\ &= \frac{M_{\mathrm{cat}} k_f K_{aa} \left(a_{aa} a_{ipa} - \frac{K_w}{K K_{aa}} a_{\mathrm{ester}} a_w \right)}{\left(1 + K_{aa} a_{aa} + K_w a_w \right)} \quad (6) \end{aligned}$$

or

$$\begin{aligned} r_i &= n \frac{\mathrm{d}x_i}{\upsilon_i \mathrm{d}t} \\ &= \frac{M_{\mathrm{cat}} k_f K_{ipa} \left(a_{aa} a_{ipa} - \frac{K_w}{K K_{ipa}} a_{\mathrm{ester}} a_w \right)}{\left(1 + K_{ipa} a_{ipa} + K_w a_w \right)} \quad (7) \end{aligned}$$

Equations (6) and (7) will be referred to as the ER_{aa} and the ER_{ipa} models, respectively, so as to specify the reactant being adsorbed.

The LH model: In this case, the surface reaction occurring between adsorbed acetic acid with adsorbed 2-propanol is the rate-controlling step forming adsorbed water and ester molecules on the surface of the catalyst. This is a dual site reaction which can be mathematically represented as

$$\begin{aligned} r_i &= n \frac{\mathrm{d}x_i}{\upsilon_i \mathrm{d}t} \\ &= \frac{M_{\mathrm{cat}} k_f K_{aa} K_{ipa} \left(a_{aa} a_{ipa} - \frac{K_w K_{\mathrm{ester}}}{K K_{aa} K_{ipa}} a_{\mathrm{ester}} a_w \right)}{\left(1 + K_{aa} a_{aa} + K_{ipa} a_{ipa} + K_{\mathrm{ester}} a_{\mathrm{ester}} + K_w a_w \right)^2} \end{aligned}$$

$$(8)$$

where K_{ipa}, K_{aa}, K_{ester}, and K_w represent the adsorption equilibrium constants for 2-propanol, acetic acid, 2-propyl acetate, and water, respectively.

The ML model: Here too, the surface reaction occurring between adsorbed acetic acid with adsorbed 2-propanol is the rate-controlling step. However, water is found to have a very strong affinity for cation exchange resins [6,20]; Lee et al. [19] and Gangadwala et al. [23] were able to improve their kinetic predictions by introducing an exponent α to the activity of water in the rate expression. This dual site reaction can be mathematically represented as

$$
r_i = n\frac{dx_i}{\upsilon_i dt}
$$
$$
= \frac{M_{cat}k_f K_{aa}K_{ipa}\left(a_{aa}a_{ipa} - \frac{K_w K_{ester}}{K K_{aa}K_{ipa}}a_{ester}a_w^\alpha\right)}{\left(1 + K_{aa}a_{aa} + K_{ipa}a_{ipa} + K_{ester}a_{ester} + K_w a_w^\alpha\right)^2}
$$
$$(9)$$

Pöpken model (*PP Model*): For the esterification of methanol and acetic acid over Amberlyst 15, Pöpken et al. [20] successfully used a model of the form shown below:

$$
r_i = n\frac{dx_i}{\upsilon_i dt} = \frac{M_{cat}k_f\left(a'_{aa}a'_{ipa} - \frac{a'_{ester}a'_w}{K}\right)}{\left(a'_{aa} + a'_{ipa} + a'_{ester} + a'_w\right)^2} \quad (10)
$$

where

$$
a'_i = \frac{K_i a_i}{M_i} \quad (11)
$$

and M_i denotes the molar mass of component i.

Equation (10) was obtained by coupling the power law form kinetic equation shown below:

$$
r_i = n\frac{dx_i}{\upsilon_i dt} = M_{cat}k_f\left(x_{aa}^s x_{ipa}^s - \frac{x_{ester}^s x_w^s}{K}\right) \quad (12)
$$

where

$$
x_i^s = \frac{m_i^S/M_i}{\sum_j \left(m_j^S/M_j\right)} \quad (13)
$$

represents the mole fractions of the components in the adsorbate phase and m_i^S is the adsorbed mass of component i. With an adsorption-based model obtained by assuming Langmuir-type adsorption based on mass, a relationship of the type shown

below is given for the mass coverage, m_i^S/m^S:

$$
\frac{m_i^S}{m^S} = \frac{K_i a_i}{1 + \sum_j K_j a_j} \quad (14)
$$

where m^S is the total adsorbed mass.

Pöpken et al. [20] used adsorption equilibrium constants fitted to experimentally measured sorption data in describing the reaction kinetics. However, in this work, the adsorption equilibrium constants along with the other kinetic constants were fitted to the measured kinetic data using Eq. (10) (the PP model). Therefore, there are some differences in the application of the PP model in the original work of Pöpken et al. [20] and this work.

In order to study only the kinetics of a system, diffusion effects should be absent. For heterogeneous solid–liquid catalytic systems, there exist two types of diffusion limitations: one across the interface between the bulk of the liquid phase and the catalyst surface (external diffusion limitations) and the other inside the solid particles of the catalyst (internal diffusion limitations). Carrying out the kinetic runs at sufficiently high, experimentally determined optimum agitation rates ensures absence of external diffusion limitations. For determining internal diffusion limitations on the overall reaction rate, the Weisz Prater criterion [39] is usually used [12,16,26]. The criterion focuses on calculating the parameter shown below; with the value of this parameter determining the significance of the internal diffusion:

$$
C_W = \frac{-r'_A(obs)\rho_p R_c^2}{D_e C_{li}} \quad (15)
$$

where r'_A is the reaction rate at a given time in mol/g of catalyst/s, ρ_p is the catalyst density in g/cc, R_c in cm is the ratio of catalyst pellet volume to catalyst pellet external surface area in cm, C_{li} is the limiting reactant concentration in the mixture at a given time in mol/cc, and D_e is the effective diffusivity in cm^2/s calculated as

$$
D_e = \xi_v^2 D_{lm} \quad (16)
$$

where ξ_v is the void fraction and D_{lm} is the diffusivity of the limiting reactant in the mixture in cm^2/s. The Perkins and Geankoplis method [40] was used to

calculate the multicomponent diffusivity D_{lm}:

$$D_{\text{lm}}\eta_m^{0.8} = \Sigma \sum_{\substack{j=1 \\ j \neq l}}^{n} x_j D_{lj} \eta_j^{0.8} \qquad (17)$$

where x_j is the mole fraction of component j; η_m and η_j are the viscosities in cp of the mixture and component j, respectively; and D_{lj} is the binary diffusivity of limiting reactant in component j. η_m and η_j can be determined by the HYSYS version 3.1 program, using the Peng–Robinson–Stryjek–Vera (PRSV) equation of state.

EXPERIMENTAL

Chemicals

The reactants used 2-propanol (catalogue # 59300) and acetic acid (catalogue # 27225) were pure grade products of Fluka and Riedel-de Haen, respectively, and were used as such. GC analysis showed their respective purity values to be greater than 99.8%. For titration, the alkali used was sodium hydroxide volumetric-standard, 0.1024 N solution in water of Aldrich Chemical Co. (catalogue # 31948-1). The concentration of the alkali solution was confirmed by back titrating it with a freshly prepared solution of potassium hydrogen phthalate of known concentration. The potassium hydrogen phthalate was obtained from Aldrich (catalogue # 17992-2) and had a purity of greater than 99.9%. The catalysts used, Dowex 50Wx8-400 (catalogue # 217514), Amberlite IR-120 (catalogue # 216534), and Amberlyst 15 (catalogue # 216380) were obtained from Aldrich and had the properties shown in Table I.

Kinetic Runs

All the kinetic studies were performed in a LabMax reactor, supplied by Mettler-Toledo AG. Figure 1 is a schematic diagram of the apparatus used. The 1-L reactor vessel, which is made of glass, is jacketed and equipped with a speed controllable mechanical agitator and a temperature probe. Heat exchange oil is pumped through the outer jacket of the vessel to control the temperature of the reaction mixture. The reaction contents are not allowed to exceed 500 mL to ensure uniform mixing. This works out to about 4 mol of the reactants in most cases. The calculated amount of the acid along with previously dried and weighed catalyst is added to the reactor, and the temperature of the reactor is raised to that of the required reaction temperature. All the three catalysts were vacuum dried at 343 K for 48 h. Drying at temperatures significantly higher than this temperature ($\geq$373 K) could lead to the loss of active sulfonic acid sites on the catalysts. Drying was carried out till two consecutive weight readings were the same. The alcohol is separately preheated to the reaction temperature, and at time "zero" the required amount is poured into the reactor. Two milliliter samples were withdrawn every 15 min during the first hour; every 30 min during the second hour; and then every hour for the next 2 h. These samples were titrated against standard NaOH solution of known normality to determine the acetic acid present at each stage. The reproducibility of the titration results was found to be $\pm$1.5%.

The kinetic runs were carried out at three different temperatures (303, 323, and 343 K), three different acid to alcohol molar ratios (the rounded values equal 0.5, 1, and 2), and three different catalyst loadings (20, 40, and 60 g/L) while agitating the mixture at 900 rpm.

Table I Properties[a] of the Cation Exchange Resins Used

	Dowex 50Wx8-400	Amberlite IR-120	Amberlyst 15
Manufacturer	Dow Chemical Co.	Rohm & Haas	Rohm & Haas
Supplier	Aldrich	Aldrich	Aldrich
Catalogue #	217514	216534	216380
Polymer type	Gel-type	Gel-type	Macroreticular
Matrix type	Styrene-divinyl benzene (DVB)	Styrene-divinyl benzene (DVB)	Styrene-divinyl benzene (DVB)
Functional group	Sulphonic acid	Sulphonic acid	Sulphonic acid
Standard ionic form	H+	H+	H+
Total exchange capacity, meq/mL	1.7	1.9	1.8
Cross linking, % DVB	8	8	20
Moisture content, % mass	54	45	<1.6
Maximum operating temperature, °C	150	120	120
Particle size range, mm	0.04–0.07	0.30–1.20	0.30–1.20

[a] As reported by the manufacturer.
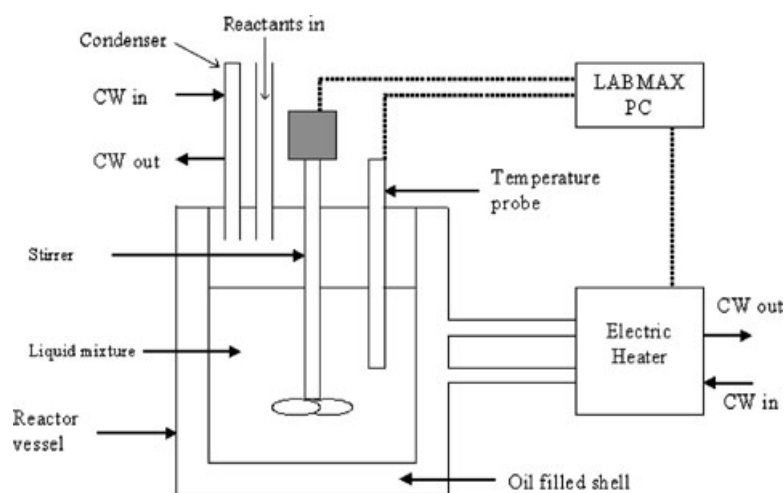
Figure 1   Schematic diagram of the apparatus used to study the kinetics of the reaction system.

Some runs were also carried out at speeds of 50, 200, and 500 rpm to determine the optimum speed for the reactions.

Equilibrium Runs

The equilibrium runs were carried out in 80 cc glass cells having outer glass jackets through which water from a circulating water bath, with temperature control, flows. The glass stoppers for the cells were fitted with smaller diameter stoppers at the top. This facilitated removal of the reaction sample by thin graduated pipettes by removing only the small upper stopper. The reaction volume was not allowed to exceed half the volume of the cells. Equimolar amounts (around 0.2 mol each) of acetic acid and alcohol, along with 1% by volume of concentrated sulfuric acid are allowed to react in the cells till equilibrium is reached (as evidenced by the absence of any change in the amount of alkali required to neutralize the acid present in 0.1 mL of the withdrawn sample). Samples were withdrawn 6, 12, 24, and 48 h from the start of the reaction. The reaction temperatures studied were 303, 323, and 343 K.

RESULTS AND DISCUSSION

Diffusion Considerations

External Diffusion Considerations: Effect of Agitation. To determine the optimum agitation speed, four runs were carried out at an acid to alcohol molar ratio of 1, temperature of 323 K, Amberlyst 15 loading of 40 g/L, and at variable stirrer speeds of 50, 200, 500, and 900 rpm. Figure 2 is a plot of the conversion of the acetic acid versus time at these different speeds. It

is seen that the rate of the reaction as followed by the conversion of acetic acid is the same when the mixture is agitated at speeds of 500 as well as 900 rpm. This indicates the absence of external mass transfer limitations above 500 rpm. Therefore, all experiments were conducted at 900 rpm. Interestingly, Kirbaslar et al. [21] and Gangadwala et al. [23] also carried out their kinetic studies at comparable stirrer speeds of 800 and 1000 rpm, respectively, since they found external
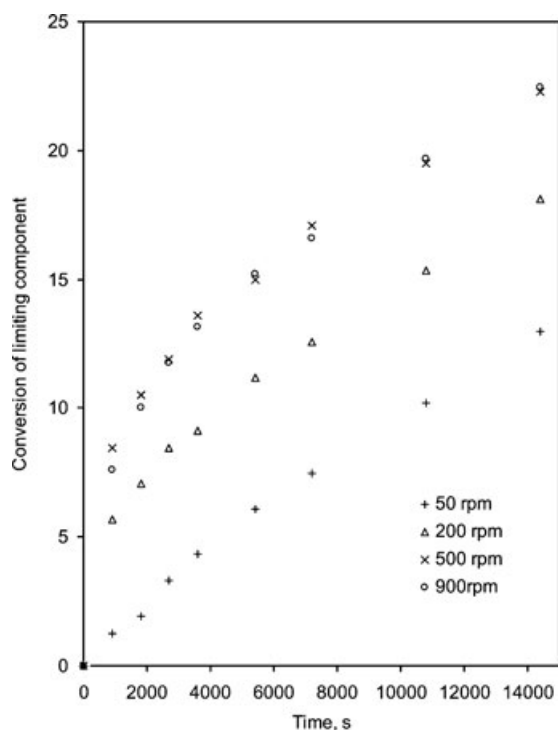
Figure 2   Effect of stirrer speed on conversion at 323 K, acid to alcohol molar ratio of 1, and catalyst loading of 40 g/L, for systems catalyzed by Amberlyst 15.

diffusion limitations to be absent at these speeds. Surprisingly, Xu and Chuang [5] found no effect on methyl acetate production rate while working at much lower stirrer speed ranges (160–760 rpm). This could be due to the fact that the viscosity of their reaction system is lower than that in this study as they studied the batch esterification of methanol with dilute acetic acid (water is less viscous than acetic acid). These observations are in line with the work of Chakrabarti and Sharma [33] wherein it has been established that external diffusion does not generally control the overall rate in ion exchange resin catalyzed processes unless the viscosity of the reactant mixture is very high or the speed of agitation is very low.

Internal Diffusion Considerations: Weisz Prater Criterion. The Weisz Prater criterion was calculated according to Eq. (15) for the initial stage of the kinetic runs (15 min). The detailed results for the different systems are shown in Table II. The value of this criterion was found to be much less than 1 ($\leq$5.0E-4, $\leq$1.9E-2, and $\leq$4.2E-2 for the systems catalyzed by Dowex 50Wx8-400, Amberlite IR-120, and Amberlyst 15,

Table II Significance of Pore Diffusion for the Different Systems

Experimental Parameters[a]	D_{eff} (cm²/s)	C_w^b
System catalyzed by Dowex 50Wx8		
40/323/1	5.09E-06	1.45E-04
20/323/1	5.09E-06	2.79E-04
60/323/1	5.09E-06	9.26E-05
40/323/0.5	3.38E-06	1.12E-04
40/323/2.0	6.64E-06	4.98E-04
40/303/1	3.27E-06	1.30E-04
40/343/1	7.48E-06	1.95E-04
System catalyzed by Amberlite IR-120		
40/323/1	5.09E-06	1.30E-02
20/323/1	5.09E-06	1.87E-02
60/323/1	5.09E-06	8.70E-03
40/323/0.5	3.36E-06	1.23E-02
40/323/2.0	6.75E-06	1.40E-02
40/303/1	3.25E-06	1.63E-02
40/343/1	7.48E-06	1.73E-02
System catalyzed by Amberlyst 15		
40/323/1	1.50E-06	1.98E-02
20/323/1	1.50E-06	3.37E-02
60/323/1	1.50E-06	1.32E-02
40/323/0.5	1.00E-06	1.40E-02
40/323/2.0	1.95E-06	4.20E-02
40/303/1	9.62E-07	2.58E-02
40/343/1	2.19E-06	2.31E-02

[a] First number: catalyst loading in g/L, second number: temperature in K, third number: acid to alcohol mole ratio.
[b] According to Eq. (15).

respectively) indicating the absence of internal mass transfer diffusion for all cases. The respective values of this criterion for the systems catalyzed by Dowex 50 Wx8-400, Amberlite IR-120, and Amberlyst 15 are found in the range from 9.3E-5 to 5.0E-4, 8.7E-3 to 1.9E-2, and 1.3E-2 to 4.2E-2. These values are somewhat in the same order as the values reported by Bart et al. [16] (from 1.3E-4 to 1E-2) and Krishnaiah and Rao [12] (from 6E-4 to 1.7E-3) while studying the esterification of the primary alcohol, propyl alcohol with acetic acid over Dowex monosphere 650 C and Dowex 50Wx8, respectively.

Equilibrium Studies

The esterification runs at 303, 323, and 343 K, acid to alcohol ratio of 1 and 1% by volume of concentrated sulfuric acid yielded the equilibrium mole fractions of the acid, alcohol, ester and water. Equilibrium was reached after 12 h for the reaction at 303 K and after 6 h for the reactions at 323 and 343 K. The corresponding equilibrium acid mole fractions were found to be 0.180, 0.185, and 0.189, respectively. The equilibrium constant, K, at the different temperatures for this esterification reaction was determined by the equation shown below:

$$K = \frac{(x_{\mathrm{ester}})_{\mathrm{eq}}(x_w)_{\mathrm{eq}}}{(x_{aa})_{\mathrm{eq}}(x_{ipa})_{\mathrm{eq}}} \frac{\gamma_{\mathrm{ester}}\gamma_w}{\gamma_{aa}\gamma_{ipa}} \qquad (18)$$

where $(x_i)_{\mathrm{eq}}$ is the mole fraction of component i at equilibrium and γ_i is the activity coefficient of component i at equilibrium determined by the UNIFAC model.

The equilibrium constants were found to decrease with increase in temperature; a trend which has been observed by Xu and Chuang [5] while studying the esterification of methyl alcohol with acetic acid. However, Lee et al. [18] and El-Naomany et al. [14] while studying the equilibrium of the reaction of acetic acid with amyl alcohol and isobutanol, respectively, found the equilibrium constant values to increase marginally with increase in temperature. In the current study at 303, 323, and 343 K, the equilibrium constant was found to have values of 29.4, 26.0, and 23.0, respectively. The plot of the natural logarithm of equilibrium constant values as a function of the inverse of absolute temperature is shown in Fig. 3. The ln(K) by $1/T$ plot gives a good linear fit with an R_{fit}^2 value of 0.99, and the equation obtained is shown below:

$$K = 3.48128 \exp\left(5402.5/R_g T\right) \qquad (19)$$

The decrease in K values with increase in temperature shows that this esterification is exothermic. The small value of the heat of reaction, -5.4 kJ/mole, is
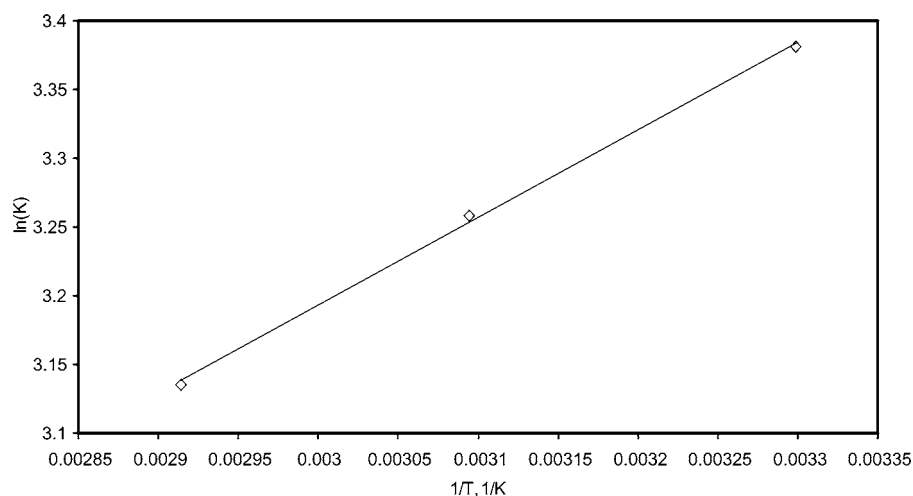
Figure 3 Natural logarithm of equilibrium constant as a function of inverse temperature.

an indication of the equilibrium constant not being a strong function of temperature. This value is comparable to the value of -2 kJ/mol obtained by Xu and Chuang [5] for the esterification of methanol with acetic acid. Interestingly, though El-Naomany et al. [14] and Lee et al. [18] found the reaction studied by them to be endothermic in nature; they too found the magnitude of the heat of the reaction to be small (8.9 and 6.4 kJ/mole, respectively). In general, the equilibrium constant in most esterification reactions is a weak function in temperature because of small values of involved heats of reaction. In fact, Lee and Kuo [41] found the equilibrium constants to be independent of temperature measured over the boiling temperature range of the mixture at atmospheric pressure. For the 2-propyl alcohol/acetic acid esterification system, Agreda et al. [42] found the equilibrium constant for the esterification of methyl alcohol with acetic acid also to be independent of temperature.

In this study, we have compared the performance of several surface reaction models in which different components are assumed to be adsorbed to different extents on the catalyst surface. The simplest model used, the PH model, assumes reaction homogeneity and its rate equation (Eq. (2)) calls for a homogeneous reaction equilibrium constant (K). This K term has been uniformly maintained in the reaction rates of all the models (ER, LH, ML, and PP) to enable direct comparison of the component adsorption equilibrium constants predicted by these models. Since the functional group in the case of all the heterogeneous catalysts studied is sulfonic acid, it was thought to be advantageous to obtain the required K values from a reaction system catalyzed homogeneously by an equivalent amount of sulfuric acid (the small amount of sulfuric acid used equals 1% v/v).

Reaction Kinetics

The absence of both external and internal diffusion limitations indicates that under the reaction conditions studied, kinetics rather than mass transfer is the rate-controlling step.

Effect of Reaction Temperature. At each temperature, the reaction rate is found to decrease with increase in reaction time. This behavior is due to the decrease in the driving force for the forward reaction leading to ester formation (with time the concentration/activities of the reactants decreases and that of the products increases) and also due to the detrimental effect [33] on the reaction rate of the water formed during the course of the reaction. Figure 4 is a plot of the conversion of the limiting component with time at 343, 323, and 303 K. This figure shows that for each of the three catalysts studied, increase in temperature has the effect of increasing the conversion. A similar trend has been observed for cation-exchange resin catalyzed esterification studies by other workers [5,7,12,14,16,21,26,27] also. Furthermore, Fig. 4 also shows that at each of the temperature studied, the enhancement in conversion with increase in temperature becomes more pronounced as the reaction time increases.

At the lowest temperature studied, 303 K, all the three catalysts exhibit comparable kinetics during the early stages of the reaction. During the last 2 h of the reaction, Dowex performs slightly better than Amberlite and Amberlyst. At 323 K, the catalytic activities of the two gel-type catalysts, Dowex and Amberlite, are comparable to one another, and both of them perform better than Amberlyst especially after the initial stage of the reaction. This indicates that the decrease in the rate of the reaction with time is less
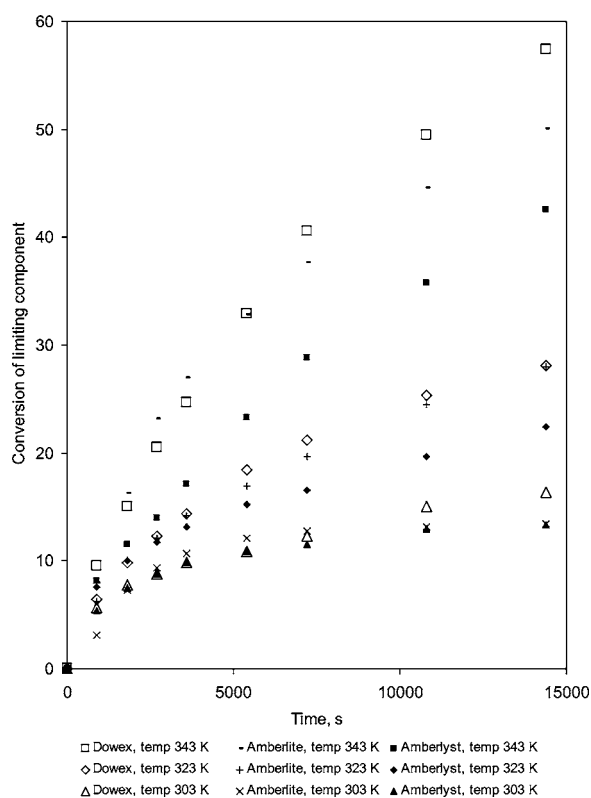
Figure 4 Effect of temperature on conversion at acid to alcohol molar ratio of 1 and catalyst loading of 40 g/L.

exhibited by Dowex at a reaction time of 4 h and a temperature of 343 K. From Fig. 4, it is also seen that in general, increasing the temperature at any point of reaction time has the effect of increasing the kinetics of the gel-type catalysts to a larger extent than that of the macroreticular catalyst. This observation is also probably linked to the differences in the impact the formed water has on the gel versus the macroreticular catalyzed systems. The above observations clearly show that the effect of increasing temperature on reaction kinetics depends both on the type of catalyst as well as the reaction time.

Effect of Acid to Alcohol Molar Ratio. Figure 5 shows the effect of initial acid to alcohol molar ratio on conversion for all the three catalysts. For the Dowex-catalyzed systems, increasing the acid to alcohol ratio from 0.5 to 1 leads to higher conversions after the first half an hour of reaction. A further increase in the molar ratio from 1 to 2 (excess of acid) leads to a more significant increase in conversion. In general, increasing the acid to alcohol molar ratio, increases the conversion of the limiting reactant. This shows that under the conditions studied, the reaction kinetics can be increased by using an excess of the acid rather than the secondary alcohol. For the Amberlite system also, the increase in acid mole fraction enhances the conversion significantly.

pronounced for the systems catalyzed by gel-type resins than those catalyzed by macroreticular catalysts. Water formed in the course of the reaction appears to influence the gel-type and macroreticular resin catalyzed systems to different extents. This appears logical in view of the work of Toteja et al. [43] wherein behavioral differences between the water present in the gel phase and in the pores of the macroreticular Amberlyst-15 have already been established. This influence of water is also observed at 343 K. At this temperature, the rates of the reaction are found to be considerably higher for the gel-type catalysts, Amberlite and Dowex, than the macroreticular catalyst, Amberlyst, all along the course of the reaction. In general, at 323 and 343 K, the water formed during the course of the reaction appears to decrease the activity of the macroreticular-catalyzed rather than gel-type resin-catalyzed system to a greater extent. It is interesting to note that Lee et al. [19] also found Dowex 50Wx8-100, a gel-type catalyst to be more active than Amberlyst 15, a macroreticular catalyst, at 353 K for the esterification of acetic acid with amyl alcohol at 343 K.

At 343 K and reaction times of 2, 3, and 4 h Dowex is found to give higher conversions than Amberlite. The largest conversion (57%) obtained in this study is

Figure 5 Effect of acid to alcohol molar ratio on conversion at 323 K and catalyst loading of 40 g/L.

Here, too, increasing the ratio from 1 to 2 is more beneficial than increasing it from 0.5 to 1. On the other hand, for the Amberlyst catalyzed systems raising the ratio from 0.5 to 1 did not cause any significant kinetic changes; however, raising the ratio from 1 to 2 significantly enhanced the kinetics as reflected by the conversion values.

In general, the increase in the acid mole fraction results in the increase of the conversion of the limiting components in the initial as well as the later stages. A similar trend has been observed by Krishnaiah and Rao [12] while studying cation exchange catalyzed esterification reactions. Mazotti et al. [6] found the change in the reaction rate with change in the acid to alcohol mole ratio to be a consequence of the selective sorption of the reactants on the resin. Earlier workers [6,7] have found the initial reaction rate to increase, reach a maximum, and then decrease with increase in acid to alcohol mole ratio. Their work has established that initial rates can increase or decrease with increase in the acid to alcohol mole ratio depending on the overall alcohol concentration, the overall acid concentration, and the reaction temperature. Interestingly, Kirbasler et al. [21] found the conversion to decrease with increase in the acid to alcohol ratio.

For all the three catalysts, the impact on conversion of change of molar ratio of reactants from a value of 0.5 to 1 is not as remarkable as when the mole ratio is increased from 1 to 2. This shows that the rate does not increase linearly with initial molar ratio of reactants.

The trends in changes in conversion with step-by-step change in the acid to alcohol ratios are similar for Dowex and Amberlite, both of which are gel-type catalysts. This indicates a greater degree of similarity in their respective reaction kinetics as compared with that of Amberlyst. Further along this work, during kinetic data fitting this observation is found to hold true.

It is interesting to note that at acid to alcohol molar ratios of 2, Amberlyst is found to give the highest conversions at reaction times of 15, 90, and 120 min; Dowex gives the highest conversions at reaction times of 30, 45, and 60 min; while Amberlite gives the highest conversions at reaction times of 180 and 240 min. This clearly indicates that besides the initial reactant mole ratio, the performance of these three catalysts relative to one another depends on the reaction time also.

Effect of Catalyst Loading. Figure 6 shows the effect of catalyst loading on conversion for all the three catalysts. As has been observed by previous workers [12,13,16,21], for all the three catalysts, increasing the catalyst concentration is found to increase the conversion for all the three catalysts. Such a behavior is expected since increasing the catalyst concentration in-
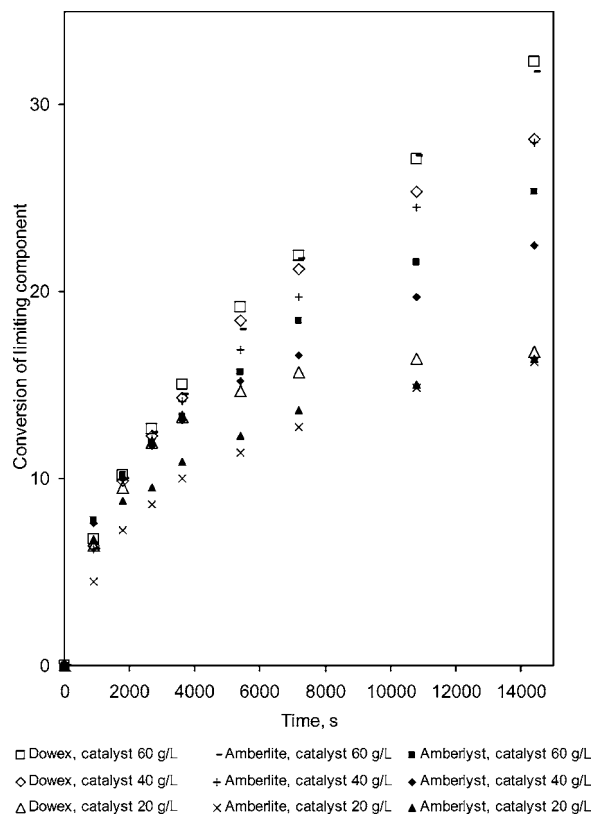
Figure 6 Effect of catalyst loading on conversion at 323 K and acid to alcohol molar ratio of 1.

creases the number of resin functional groups, and this will cause an increase in the reaction rates [13]. At longer reaction times, the influence of thermodynamic limitations will be dominant and the effect of catalyst concentration on reaction rates is expected to become less pronounced. Furthermore, it is found that for all the three catalysts, the increase in conversion is more significant when the catalyst concentration is raised from 20 to 40 g/L than when it is raised from 40 to 60 g/L. Similar trends have also been observed by Bart et al. [16] and Kirbaslar et al. [21].

At 20 g/L catalyst loading and after the first half an hour of reaction, Dowex does significantly better than Amberlyst, which in turn performs slightly better than Amberlite. However, 4 h after the start of reaction, no appreciable differences in catalyst kinetics are observable. At the 40 and 60 g/L level, Dowex and Amberlite exhibit somewhat comparable kinetics throughout the reaction and both these catalysts perform significantly better than Amberlyst.

It is interesting to note that even for the Dowex-catalyzed system studied, at catalyst concentrations of 60 g/L the conversion values obtained (15, 22, 27, and 32% at 1, 2, 3, and 4 h of reaction time, respectively) are much lower than the values obtained (23, 37, 43, and

50% at 1, 2, 3, and 4 h of reaction time, respectively) by Krishnaiah and Rao [12] using half the catalyst loading (30 g/L) while studying the Dowex 50Wx8 catalyzed esterification of acetic acid with n-propanol, which is an unhindered geometric isomer of the alcohol used in this study. This shows that the steric factors associated with the alcohol have a great bearing on the reaction kinetics.

At both 40 and 60 g/L catalyst loadings, the kinetics of all the three catalysts are comparable during the early stage of the reaction (upto 45 min). A similar observation has been made by Gangadwala et al. [23]. During the first hour of reaction, they found the activity of Amberlyst 15 to be very close to that of Amberlite IR-120 at comparable catalyst concentrations of around 60 g/L. This suggests that factors like high catalyst concentrations can mask the influence of catalyst nature under certain reaction conditions.

Development of a Kinetic Model

Predicting System Nonideality with UNIFAC. The UNIFAC equation (Eq. (3)) was used to account for the nonideality present in the system. Table III shows the UNIFAC groups into which the components were split, and the corresponding group volume (R) and group area (Q) parameter values used. Linearly temperature dependant binary interaction parameters reported by earlier workers [44] were used to predict the activity coefficients at the different temperatures studied. During the course of the reaction, the activity coefficients of 2-propanol, 2-propyl acetate, and water were found to increase and the activity coefficient of acid was found to decrease. The change in the activity coefficient of the ester was found to be relatively small. For the system catalyzed by Amberlyst 15 at 323 K, at an acid to alcohol molar ratio of 1, catalyst loading of 40 g/L, the values at the beginning of the run were found to be 0.95, 0.90, 1.73, and 2.00 for acetic acid, 2-propanol, 2-propyl acetate, and water, respectively. These values are comparable to the UNIQUAC predicted activity coefficient values obtained by Maki-Arvela et al. [17]

Table III The UNIFAC Groups Present in the Different Components and Their R and Q Values

	CH$_3$	CH	COOH	CH$_3$COO	OH	H$_2$O
Acetic acid	1	0	1	0	0	0
2-Propanol	2	1	0	0	1	0
2-Propyl acetate	2	1	0	1	0	0
Water	0	0	0	0	0	1
R	0.9011	0.4469	1.3013	1.9031	1	0.92
Q	0.848	0.228	1.224	1.728	1.2	1.4

(0.98, 0.94, 1.37, and 1.83), while studying the esterification of 1 mol of acetic acid with 1 mol of methanol. These authors also found the activity coefficient of the alcohol, ester, and water to increase and that of acetic acid to decrease with increase in reaction time.

Predicting the Most Suitable Reaction Mechanism for the Different Catalysts. The heterogeneous kinetic models, namely the pseudohomogeneous model (PH), the two Eley Rideal models (ER), Langmuir Hinshelwood model (LH), modified Langmuir Hinshelwood model (ML), and Pöpken's modified power law model (PP) discussed in the earlier section on "Theory" and represented by Eqs. (2) and (6)–(10) were applied to correlate the kinetic data available for different temperatures, catalyst loadings, and mole ratios of acetic acid to 2-propanol. The temperature-dependent K values as expressed by Eq. (19) were used in the different kinetic expressions (representing the PH, ER, LH, MLH, and PP models). Fitting the data to the models and determining the corresponding model parameters was done using Mathematica's Statistics "NonlinearFit" function. The aim of the data-fitting procedure is to minimize the mean-square differences between calculated values of the rate with the rate obtained directly from the experimental data using the differential method. Mathematically this can be expressed by the following equation:

$$\min_{p} \phi = \sum_{\text{all data samples}} (r_{\text{cor}} - r_{\text{exp}})^2 \qquad (20)$$

The outcome of fitting the kinetic data of the studied system to each of the six equations is shown in Tables IV and V. The respective tables show the values of the parameters/constants generated and the mean relative error percentage (Eq. (21)), between the predicted and experimental acid mole fractions obtained under the different reaction conditions, individually as well as collectively.

$$\text{Mean Relative Error} = \frac{\sum\limits_{\text{all data samples}} \frac{\left| x_{\text{exp}} - x_{\text{pred}} \right|}{x_{\text{exp}}}}{n_{\text{sample}}} * 100$$

$$(21)$$

Dowex 50Wx8-Catalyzed System. All the models were able to predict the kinetics with overall mean relative errors less than or equal to 5.1% as can be seen from Table V. Figure 7 is a plot of the experimental as well as predicted (by all the models) conversion values for the Dowex-catalyzed esterification at 323 K, catalyst loading of 60 g/L, and acid to alcohol molar ratio of 1.

Table IV Kinetic Parameters Generated for the Different Systems with Different Models

Model (Equation #)	A_f (mol/g/s)	E_f (J/mol)	k_f, (mol/g/s)			K_{aa}	K_{ipa}	K_{ester}	K_w
			303 K	323 K	343 K				
			System catalyzed by Dowex 50Wx8						
PH (Eq. (2))	1.99E+04	55700	5.0E-06	2.0E-05	6.6E-05	–	–	–	–
ER$_{aa}$ (Eq. (6))	1.00E+04	51500	1.3–05	4.7E–05	1.4E-04	1.24	–	–	9.93
ER$_{ipa}$ (Eq. (7))	1.90E+06	67323	4.8E-06	2.5E-05	1.1E-04	–	2.70	–	12.10
LH (Eq. (8))	1.74E+06	60000	8.0E-05	3.5E-04	1.3E-03	0.22	3.95	0.002	12.00
ML (Eq. (9))	1.27E+05	57000	1.9E-05	7.7E-05	2.7E-04	1.01	2.00	0.01	12.00
PP(Eq. (10))	1.00E+04	51500	1.3E-05	4.7E-05	1.4E-04	1.04	4.57	0.01	3.00
			System catalyzed by Amberlite IR-120						
PH (Eq. (2))	7.18E+04	58973	4.9E-06	2.1E-05	7.6E-05	–	–	–	–
ER$_{aa}$ (Eq. (6))	1.94E+05	60000	8.9E-06	3.9E-05	1.4E-04	1.30	–	–	9.70
ER$_{ipa}$ (Eq. (7))	3.16E+04	56686	5.4E-06	2.2E-05	7.4E-05	–	3.01	–	9.20
LH (Eq. (8))	2.33E+06	65080	1.4E-05	7.0E-05	2.9E-04	1.03	4.37	2.2E-05	8.62
ML (Eq. (9))	8.67E+05	59000	5.9E-05	2.5E-04	9.1E-04	0.19	2.00	0.11	12.00
PP(Eq. (10))	7.71E+04	55000	2.6E-05	9.9E-05	3.3E-04	2.00	3.00	0.10	10.00
			System catalyzed by Amberlyst 15						
PH (Eq. (2))	1.43E+05	61500	3.6E-06	1.6E-05	6.2E-05	–	–	–	–
ER$_{aa}$ (Eq. (6))	5.69E+06	63000	7.9E-05	3.7E-04	1.5E-03	0.05	–	–	0.82
ER$_{ipa}$ (Eq. (7))	5.67E+06	63109	7.6E-05	3.6E-04	1.4E-03	–	0.06	–	0.88
LH (Eq. (8))	3.58E+05	60000	1.6E-05	7.2E-05	2.6E-04	1.65	2.25	1.0E-05	16.59
ML (Eq. (9))	1.26E+05	59000	8.6E-06	3.7E-05	1.3E-04	1.10	1.80	1.0E-04	11.62
PP(Eq. (10))	8.50E+06	64000	8.0E-05	3.8E-04	1.5E-03	0.17	11.74	0.09	5.24

The plot clearly shows that all the models predict the kinetics reasonably well. Even the PH model, which returns the largest error (5.1%) compared to the other models, is competent at predicting the kinetics of this system. Though this model is the least complex and has a smaller number of parameters, theoretical support for the pseudohomogeneous model [20] comes from the fact that the polymeric catalyst swells in contact with polar solvents such as water or alcohol by more than 50% of its dry volume. This facilitates diffusion in the polymer matrix and makes the polymer-bound sulfonic acid groups readily accessible for the reactants. However, this model does not take into account the different resin swelling abilities of the components. The ER_{aa}, ER_{ipa}, LH, ML, and PP models, all of which can be considered as more advanced than the PH model, since they all take into account adsorption of the components are found to predict the kinetics with slightly lower errors, as can be seen from Table V.

Table V shows that the ML model gives the lowest collective mean relative error (3.9%) indicating that while the other models are also adequate; this model is better suited for predicting the reaction kinetics under studied conditions. Furthermore, the mean relative error given by the ML model at different conditions for Dowex ranged between 1.7 and 5.8%. This means that the different effects are properly described by

this model. Moreover, Fig. 8, the parity plot for this model clearly shows that the experimental and calculated values lie close to one another. This further indicates the suitability of this model to predict the studied kinetics. It is interesting to note that Lee et al. [19] also found the ML model, though with a higher α value of 3, to be the most suitable for predicting the esterification of acetic acid with amyl alcohol over Dowex 50Wx8-100 in a fixed bed reactor. Moreover, Krishnaiah and Rao [12] while studying the esterification of propyl alcohol with acetic acid over Dowex 50Wx8 found the LH model to be the most suitable predictive model. These studies [current work, 12,19] suggest that the LH model is efficient in predicting the Dowex 50Wx8 catalyzed esterification of acetic acid with different alcohols provided appropriate corrections for the selectivity of water adsorption on the resin (by way of α values) are accounted for ($\alpha = 2$, this work; $\alpha = 3$, work of Lee et al. [19]; $\alpha = 1$, work of Krishnaiah and Rao [12]). Interestingly, when the acid is changed as in the case of the study of Dowex 50Wx8 catalyzed esterification of butanol with oleic acid by Bhatia et al. [7], the rate-determining step is found to be the surface reaction between adsorbed oleic acid and unadsorbed n-butanol, i.e., the ER model is found to be the most suited to predict kinetics. These observations seem to indicate that the type of acid and alcohol play an

Table V Mean Relative Errors (Eq. (21)) Obtained While Fitting Experimental Runs with the Different Models

Run No.	Cat Load (g/L)	Temp. (K)	Acid to Alcohol Molar Ratio	Models Tested					
				PH	ER_{aa}	ER_{ipa}	LH	ML	PP
System catalyzed by Dowex 50Wx8									
1	40	303	1	6.9	5.1	6.7	5.7	5.8	5.7
2	40	323	1	5.5	3.7	4.6	4.4	2.7	4.4
3	40	343	1	4.9	10.1	6.0	9.4	4.6	9.4
4	20	323	1	6.6	4.7	5.3	4.8	4.9	4.8
5	60	323	1	2.6	1.4	2.4	2.4	1.7	2.4
6	40	323	2	5.9	4.8	4.1	2.7	3.4	2.7
7	40	323	0.5	3.5	3.8	2.2	1.7	4.0	1.7
Collective mean relative error (%)				*5.1*	*4.8*	*4.5*	*4.5*	*3.9*	*4.5*
System catalyzed by Amberlite IR-120									
8	40	303	1	6.6	6.0	5.8	6.4	5.9	3.3
9	40	323	1	4.4	4.5	4.1	4.6	3.4	3.2
10	40	343	1	3.9	3.7	2.2	1.0	1.6	8.1
11	20	323	1	3.6	2.9	2.8	3.1	2.8	0.7
12	60	323	1	2.3	2.3	1.6	2.3	1.0	2.3
13	40	323	2	5.0	5.2	3.5	3.2	2.2	3.2
14	40	323	0.5	4.4	3.9	3.0	2.3	3.1	3.7
Collective mean relative error (%)				*4.3*	*4.0*	*3.3*	*3.3*	*2.8*	*3.5*
System catalyzed by Amberlyst 15									
15	40	303	1	5.8	5.7	5.7	4.8	6.0	5.0
16	40	323	1	4.7	4.2	4.1	3.9	6.1	2.9
17	40	343	1	4.8	3.0	3.0	2.9	2.4	3.1
18	20	323	1	5.9	5.4	5.4	4.5	6.6	4.2
19	60	323	1	3.4	2.6	2.6	2.0	3.7	1.8
20	40	323	2	7.4	7.0	6.9	6.2	7.8	2.6
21	40	323	0.5	3.7	3.4	3.3	1.8	4.4	4.4
Collective mean relative error (%)				*5.1*	*4.5*	*4.4*	*3.7*	*5.3*	*3.4*

important role in determining the number of sites involved in this heterogeneously catalyzed reaction.

The ML model predicts an activation energy of 57.0 kJ/mole (shown in Table IV) for the forward reac-

tion of acetic acid with 2-propanol over Dowex. This value seems reasonable since it is comparable to the value of 54.3 kJ/mol obtained by Krishnaiah and Rao [12], while studying the esterification of acetic acid
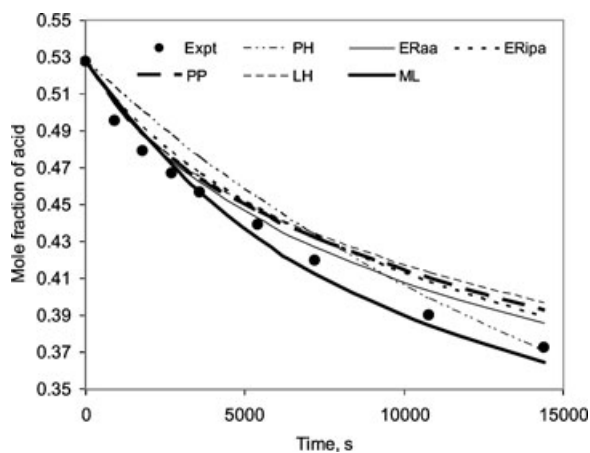
Figure 7 Comparison of experimental and predicted acid mole fractions at 323 K, acid to alcohol molar ratio of 1, and catalyst loading of 60 g/L for the Dowex 50Wx8 catalyzed system.
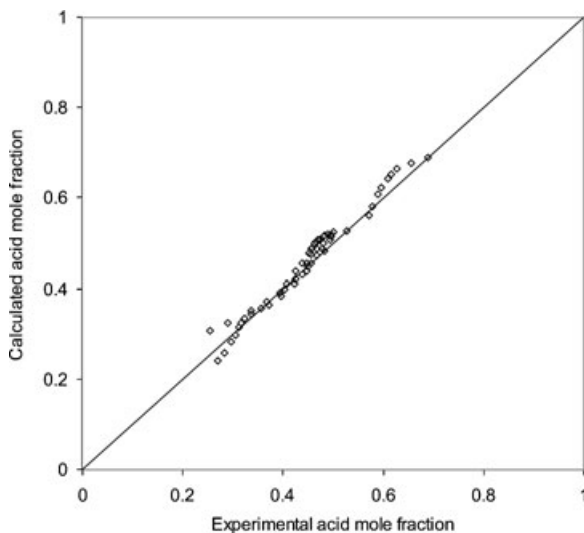
Figure 8 Parity plot for the Dowex 50Wx8 catalyzed systems using the ML model.

with propyl alcohol, which is the less hindered isomer of 2-propanol.

Table IV shows that both the LH and ML models return adsorption equilibrium constant values having the same trends, namely $K_{\text{ester}} < K_{aa} < K_{ipa} < K_w$. Though the trend for the PP model appears to be different, it is actually the same since for this model the adsorption is assumed to be mass dependent and the component activities (a_i) in Eq. (10) are multiplied by K_i/M_i and not K_i. The trend in K_i/M_i values generated by the PP model for the different components is found to be $K_{\text{ester}}/M_{\text{ester}}$ $(0.01/102 = 0.098 \times 10^{-3}$ mol/g) $< K_{aa}/M_{aa}$ $(1.04/60 = 0.017$ mol/g) $< K_{ipa}/M_{ipa}$ $(4.57/60 = 0.076$ mol/g) $< K_w/M_w$ $(3.00/18 = 0.167$ mol/g), i.e., it is the same as that generated by the LH and ML model for K_i.

The trend in the adsorption equilibrium constant is found to be the same as that of the solubility parameters of the components (the solubility parameters estimated at 298 K of 2-propyl acetate, acetic acid, 2-propanol, and water are found to be 17.15, 19.06, 23.41, and 47.81 $(\text{J/cm}^3)^{0.5}$ from the AIChE DIPPR® Database) present in this system. The proportionality between adsorption equilibrium constant and solubility parameter agrees with earlier reported work wherein it has already been established that the extent to which a component is sorbed is related to the extent to which it swells the catalyst [6]; which in turn largely depends on the ability of the component to form solvation shells around the polymer matrix [45].

Unfortunately, these trends in the adsorption equilibrium constant cannot be compared with those obtained by earlier workers using Dowex 50Wx8 as the esterification catalyst as these authors [7,12,19] did not fit their kinetic data to equations accounting for adsorption by all the components present in the system.

Amberlite IR-120 Catalyzed System. For the Amberlite-catalyzed system also all the six models were found to be adequate in predicting the reaction kinetics as indicated by the small values of their mean relative errors as shown in Table V. Figure 9 compares the experimentally obtained product conversion values with those predicted by all the models for the Amberlite catalyzed esterification at 323 K, catalyst loading of 60 g/L and acid to alcohol molar ratio of 1. For this system, the simplest model, the PH model was also efficient in predicting the involved kinetics as shown by the low value of the mean relative error returned by this model (4.3%). This is in line with the work of El-Noamany et al. [14] who was successful in predicting the Amberlite IR-120 catalyzed kinetics of acetic acid with isobutanol using the simple power law equation, the only equation tried in this published work.
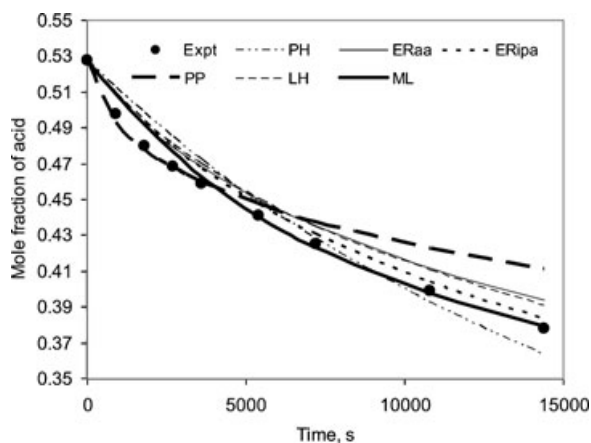
Figure 9 Comparison of experimental and predicted acid mole fractions at 323 K, acid to alcohol molar ratio of 1, and catalyst loading of 60 g/L for the Amberlite IR-120 catalyzed system.

However, in the current study, the ML model was the most efficient one with a mean relative error of just 2.8. Its efficacy is also clearly reflected in Fig. 9, which shows the closeness of the experimentally obtained kinetic data with predicted ones by the ML model. The ML model predicts the acid mole fractions for all the runs also very closely as can be seen from its parity plot (Fig. 10) having a collective mean relative error of 2.8%. For this catalyst, the mean relative error for the different conditions, using the ML model ranged between 1 and 5.9% indicating the ability of this model in describing reaction kinetics under varied conditions.

The ML model predicts an E_{act} of 59.0 kJ/mol (shown in Table IV), which seems reasonable since it
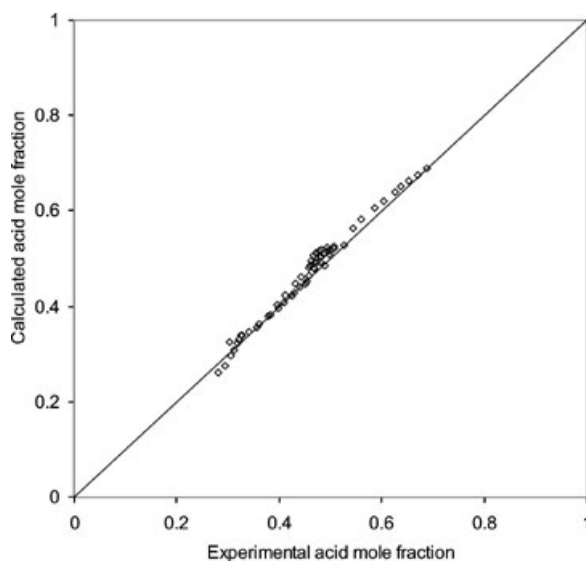
Figure 10 Parity plot for the Amberlite IR-120 catalyzed systems using the ML model.

is comparable to the value of 50 kJ/mol reported by El-Noamany et al. [14] for the Amberlite IR-120 catalyzed esterification of acetic acid with isobutanol. Table IV also shows that the PP, LH, and ML models generate component adsorption equilibrium constant with the same trends ($K_{ester}/M_{ester} < K_{aa}/M_{aa} < K_{ipa}/M_{ipa} < K_w/M_w$ for the PP model and the trend $K_{ester} < K_{aa} < K_{ipa} < K_w$ for the LH and ML models). Interestingly, the trend in the adsorption equilibrium constant for this system is also the same as that of the solubility parameters of the components present in the system as was found for the Dowex catalyzed system.

Amberlyst 15 Catalyzed System. All the six models tried, including the PH model, were effective in predicting the reaction kinetics; the mean relative error was found to be <5.3% for all of them. The adequacy of the PH model to predict the esterification kinetics on Amberlyst 15 has already been established by earlier workers [5,6,18,21,26]. However, the work of Pöpken et al. [20], Gangadwala et al. [23], and Steinigeweg and Gmehling [38] clearly shows that the use of more sophisticated models which take into account the relative adsorption of different components (like the ER, LH, ML, and PP models) does result in better predictions. In this study also, kinetic predictions improved with the use of some of the more sophisticated models, namely ER_{aa}, ER_{ipa}, LH, and PP. However, the ML model gave a slightly higher error of 5.3% as compared to 5.1% which is obtained when the PH model is used. This implies that modifying the LH equation by introducing an α term offers no advantage for this system. The PP model was selected as the representative model for this system as it gave the lowest collective mean relative error value (3.4%) as can be seen from Table V. The mean relative error, between the measured and predicted kinetics of the esterification reaction, at different catalyst loading, reaction temperature, and acid to alcohol ratio for Amberlyst ranged between 1.8 and 5.0%, proving the suitability of this model in predicting the kinetic behavior under different conditions. This model is found to predict the mole fraction of acid present in the system during the course of the reaction very close to experimental values, as can be seen from Figs. 11 and 12. It is interesting to note that Pöpken et al. [20] while studying the Amberlyst 15 catalyzed kinetics of acetic acid with methanol also found this model to be the most effective in predicting kinetics. The LH model is also found to predict the kinetics with comparable though marginally higher mean relative error.

The PP model returns an activation energy of 64.0 kJ/mol for the forward reaction. This value is comparable to the value obtained by Pöpken et al. [20] for the esterification of acetic acid with methanol (60
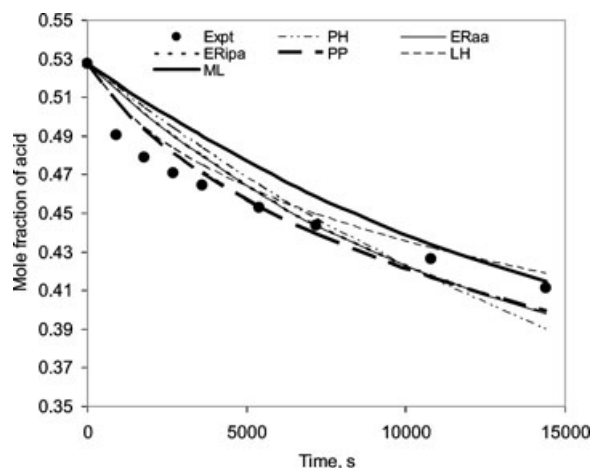
Figure 11 Comparison of experimental and predicted acid mole fractions at 323 K, acid to alcohol molar ratio of 1, and catalyst loading of 60 g/L for the Amberlyst 15 catalyzed system.
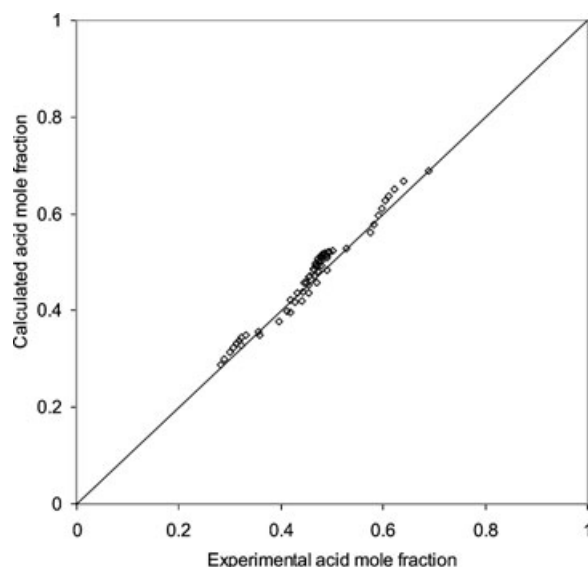
Figure 12 Parity plot for the Amberlyst 15 catalyzed system using the PP model.

kJ/mol). The PP model generates adsorption equilibrium constants (K_i/M_i) having the trend, $K_{ester}/M_{ester} < K_{aa}/M_{aa} < K_{ipa}/M_{ipa} < K_w/M_w$. Both the LH and the ML models also generate the same trends. For this system also, the trends in the component adsorption equilibrium constant are the same as those of the component solubility parameters. The trends in the component adsorption equilibrium constants also agree well with those reported by Mazotti et al. [6], Gangadwala et al. [23], and Kawase et al. [46] while studying the Amberlyst 15 catalyzed

esterification of acetic acid with ethanol, butanol, and β-phenylalcohol, respectively. However, Pöpken et al. [20] on the basis of experimentally conducted adsorption studies arrived at adsorption equilibrium constants increasing in the order of acetic acid < methyl acetate < methanol < water. Interestingly, this trend also corresponds to increase in the solubility parameter values of the components; the ester in their system, methyl acetate, has a solubility parameter value (19.35 $(J/cm^3)^{0.5}$ at 298 K reported in AIChE DIPPR® Database) greater than that of the acid in their system, acetic acid (19.06 $(J/cm^3)^{0.5}$ at 298 K reported in AIChE DIPPR® Database). This adds further weight to the finding of this study that since the component adsorption equilibrium constants are proportional to their solubility parameters, the trends in the component adsorption equilibrium constants will follow the trend of the component solubility parameters.

Comparison of the Reaction Kinetics for the Different Catalysts Used. All the six models tried were found to be adequate in predicting the reaction kinetics for the different catalysts under the different conditions studied as indicated by the low values of mean relative errors, as shown in Table V. Since all these models (Eqs. (2), (6)–(10)) use component activities predicted by the UNIFAC model to account for system nonideality, the low error values are also an indication of the success of the UNIFAC model in accounting for nonideality present in all the three catalyst systems. The predicted equilibrium mole fraction values of the reactants and products using the models best representing the kinetics of the esterification reaction catalyzed by the used ion exchange resins approach the experimentally measured equilibrium values (with slight deviation due to both experimental and modeling errors) at different points of time (beyond 4 h).

For the Dowex, Amberlite, and Amberlyst catalyzed systems, the selected models predict activation energies of 57.0, 59.0, and 64.0 kJ/mol. This shows that the gel-type catalysts, Dowex and Amberlite, have comparable activation energies and unit changes in temperature will cause less significant changes in their forward reaction rate constant, k_f, than in the case of the macroreticular catalyst, Amberlyst. This trend can easily be seen by comparing the change in k_f values when temperature is increased from 303 to 343 K. Table IV shows that the k_f value for the Dowex system increases 14 times (k_f changes from 1.9 E-5 to 2.7 E-4 mol/g/s), that of the Amberlite system increases 15 times (k_f changes from 5.9 E-5 to 9.1 E-4 mol/g/s) and that of the Amberlyst system increases 19 times (k_f changes from 8.0 E-5 to 1.5 E-3 mol/g/s). However, it should be noted that the trends observed in the E_{act} and k_f values

discussed above refer to the forward reaction only and should not be confused with the corresponding constants for the overall esterification reaction (known as the kinetic term, which will be discussed later in the manuscript). It is interesting to note here that while studying the effect of temperature on the overall reaction kinetics, the gel-type catalysts were found to exhibit greater changes in reaction kinetics with increase in temperature.

For all the three systems, the relative strengths of the component adsorption constants are found to be the same and this strength is found to increase in the order of ester < acid < alcohol < water. The similarity in the trends is to be expected since component adsorption constants depend on the ability of the components to form solvation shells in the polymer matrix, and though the three catalysts differ in their internal structure and in the degree of crosslinking they all have the same polymer matrix of styrene divinylbenzene with sulfonic acid as the functional group. The use of solubility parameter values available in the literature can be a quick and easy way to predict the relative adsorption strengths of the components present in the esterification system for systems where the catalyst contains the same polymer matrix and functional group as present in Dowex 50Wx8, Amberlite IR-120, and Amberlyst 15. Such predictions are required for the design of simulated moving bed reactors where the resin functions both as a catalyst as well as a selective sorbent [6,46].

An attempt has been made to compare the kinetics of the esterification of acetic acid with 2-propanol by comparing the contribution to the overall kinetics of the terms present in the equations found to be the most effective in predicting the reaction kinetics. The ML model, as represented by Eq. (9) (which has been found to be the most suitable for the systems catalyzed by Dowex 50Wx8 and Amberlite IR-120) as well as the PP model, as represented by Eq. (10) (found to be the most suitable for the systems catalyzed by Amberlyst 15) can be represented by the general form $\frac{(\text{kinetic term})(\text{driving force term})}{(\text{adsorption term})}$. For the ML model, the kinetic force term, the driving force term, and the adsorption term are given by the expressions

$$M_{cat}k_f K_{aa} K_{ipa}, \left(a_{aa}a_{ipa} - \frac{K_w K_{ester}}{K K_{aa} K_{ipa}} a_{ester}a_w^2 \right),$$

and

$$(1 + K_{aa}a_{aa} + K_{ipa}a_{ipa} + K_{ester}a_{ester} + K_w a_w^2)^2,$$

Table VI Comparison of Contributing Terms in the Selected Models

Time (s)	Driving Force Term	Kinetic Term (mol/s)	Adsorption Term	%Contribution of the Different Components to (Adsorption Term$^{0.5}$)				
				Acid[a]	Alcohol[b]	Ester[c]	Water[d]	G[e]
Kinetics of Dowex 50Wx8 catalyzed system predicted by the ML model								
0	0.21	1.70E-03	5.53	21.30	36.18	0.00	0.00	42.52
900	0.20	1.70E-03	5.41	20.81	35.79	0.01	0.40	42.98
1800	0.19	1.70E-03	5.38	20.18	35.12	0.02	1.57	43.10
2700	0.18	1.70E-03	5.43	19.45	34.22	0.03	3.40	42.90
3600	0.17	1.70E-03	5.56	18.64	33.15	0.04	5.73	42.43
5400	0.16	1.70E-03	5.96	16.99	30.79	0.06	11.21	40.95
7200	0.14	1.70E-03	6.53	15.44	28.43	0.07	16.91	39.14
10800	0.12	1.70E-03	7.90	12.93	24.40	0.09	27.00	35.59
14400	0.11	1.70E-03	9.39	11.12	21.37	0.09	34.78	32.64
Kinetics of Amberlite IR 120 catalyzed system predicted by the ML model								
0	0.21	1.08E-03	3.79	4.99	43.66	0.00	0.00	51.35
900	0.20	1.08E-03	3.76	4.86	43.01	0.12	0.40	51.60
1800	0.19	1.08E-03	3.78	4.70	42.05	0.24	1.56	51.45
2700	0.18	1.08E-03	3.85	4.52	40.85	0.35	3.34	50.94
3600	0.18	1.08E-03	3.97	4.33	39.49	0.44	5.57	50.17
5400	0.16	1.08E-03	4.32	3.95	36.62	0.59	10.72	48.12
7200	0.15	1.08E-03	4.76	3.60	33.84	0.70	16.02	45.84
10800	0.13	1.08E-03	5.79	3.03	29.18	0.83	25.39	41.57
14400	0.12	1.08E-03	6.89	2.63	25.70	0.89	32.67	38.11

Time (s)	Driving Force Term	Kinetic Term (mol^3/g^2/s)	Adsorption Term (mol^2/g^2)	%Contribution of the Different Components to (Adsorption Term$^{0.5}$)				
				Acid[f]	Alcohol[g]	Ester[h]	Water[i]	G[j]
Kinetics of Amberlyst 15 catalyzed system predicted by the PP model								
0	0.21	2.34E-06	0.01	1.68	98.32	0.00	0.00	0.00
900	0.20	2.34E-06	0.01	1.51	89.72	0.02	8.74	0.00
1800	0.19	2.34E-06	0.01	1.39	83.27	0.04	15.30	0.00
2700	0.18	2.34E-06	0.01	1.29	78.18	0.05	20.48	0.00
3600	0.18	2.34E-06	0.01	1.22	74.01	0.06	24.71	0.00
5400	0.17	2.34E-06	0.01	1.09	67.52	0.08	31.31	0.00
7200	0.16	2.34E-06	0.01	1.00	62.61	0.09	36.29	0.00
10800	0.14	2.34E-06	0.02	0.87	55.54	0.11	43.48	0.00
14400	0.13	2.34E-06	0.02	0.78	50.56	0.12	48.54	0.00

[a] $(K_{aa}a_{aa})$.
[b] $(K_{ipa}a_{ipa})$.
[c] $(K_{ester}a_{ester})$.
[d] $(K_w a_w^{\alpha})$.
[e] (Adsorption term$^{0.5}$ − $\{K_{aa}a_{aa} + K_{ipa}a_{ipa} + K_{ester}a_{ester} + K_w a_w^{\alpha}\}$).
[f] $(K_{aa}a_{aa}/M_{aa})$.
[g] $(K_{ipa}a_{ipa}/M_{ipa})$.
[h] $(K_{ester}a_{ester}/M_{ester})$.
[i] $(K_w a_w/M_w)$.
[j] (Adsorption term$^{0.5}$ − $\{(K_{aa}a_{aa}/M_{aa}) + (K_{ipa}a_{ipa}/M_{ipa}) + (K_{ester}a_{ester}/M_{ester}) + (K_w a_w/M_w)\}$).

while for the PP model these terms are given by the expressions

$$\frac{M_{cat}k_f K_{aa} K_{ipa}}{M_{aa} M_{ipa}},$$

$$\times \left(a_{aa}a_{ipa} - \frac{K_w K_{ester} M_{aa} M_{ipa}}{K K_{aa} K_{ipa} M_w M_{ester}} a_{ester}a_w\right),$$

and

$$\left(\frac{K_{aa}a_{aa}}{M_{aa}} + \frac{K_{ipa}a_{ipa}}{M_{ipa}} + \frac{K_{ester}a_{ester}}{M_{ester}} + \frac{K_w a_w}{M_w}\right)^2.$$

To understand how each of these terms affects reaction kinetics, the values of these terms for the run at 323 K, acid to alcohol ratio of 1 and catalyst loading of

40 g/L of solution are individually determined at each stage of the reaction and shown in Table VI. For all three catalysts, the driving force term is found to have comparable values; a drop in value from 0.21 to 0.11, from 0.21 to 0.12, and from 0.21 to 0.13 is observed for the Dowex 50Wx8, Amberlite IR-120, and Amberlyst 15 catalyzed systems, respectively, during the course of the reaction. The two gel-type catalysts are found to have comparable kinetic term values (1.70E-3 and 1.08E-3 mol/s for the Dowex and Amberlite system, respectively) while the macroreticular catalyst, Amberlyst, exhibits a kinetic term value which is smaller by around three orders of magnitude ($2.34E-6$ mol^3/g^2/s). Thus, the gel type catalysts can be considered to have higher overall apparent kinetic term as compared to the macroreticular catalyst. The adsorption term is found to increase as the reaction proceeds for all three catalysts. For each of the three catalysts the adsorption term is found to almost double during the reaction time studied. It is also interesting to note that the adsorption term of the gel-type catalysts, Dowex 50Wx8 and Amberlite IR-120, is between 2 and 3 orders of magnitude greater than that of the macroreticular catalyst, Amberlyst 15. The differences in the orders of magnitude of the kinetic terms coupled with the differences in the orders of magnitude of the adsorption terms of these catalysts result in overall reaction rates having comparable orders of magnitude even though the exact values are different. The reaction rates depend on the exact values of the kinetic, driving force and adsorption terms observed over the three different catalysts. The percentage contribution of the different components to the adsorption term is also calculated and shown in Table VI. It is clear from this table that for all these three catalysts, only the ester does not contribute significantly to the adsorption term for both types of catalyst and model used, during the entire course of the reaction. This implies that amongst all the components present the ester molecule is the most weakly sorbed, an observation which has been made by earlier workers [6,20,46]. Furthermore, it is seen that as the reaction proceeds the water adsorption term becomes the dominant one. In addition, the results in Table VI show that the adsorption term of alcohol is more significant than acid.

CONCLUSIONS

For the heterogeneously catalyzed esterification of acetic acid with 2-propanol, a stirrer speed of ≥ 500 rpm was found to be effective in eliminating external diffusion limitations. Hence, the effect of catalyst loading, temperature, and acid to alcohol molar ratio on reaction kinetics was determined at 900 rpm for all three catalyst systems. At 900 rpm, internal diffusion limitations were assessed by the Weisz Prater criterion and found to be absent for each of the three catalysts, for all different temperatures, acid to alcohol ratios, and catalyst loadings studied. The equilibrium studies indicate that this esterification reaction is mildly exothermic. Increase in temperature increases reaction kinetics and the extent of increase is found to depend on the temperature, reaction time, and catalyst used. At 323 and 343 K, the gel-type catalysts are found to catalyze the esterification reaction to a greater extent than the macroreticular catalysts. Under the studied conditions, the Dowex-catalyzed system at 343 K, acid to alcohol molar ratio of 1, and catalyst loading around a value of 40 g/L gives the highest conversion of the limiting component to the ester (57%) after 4 h of reaction.

For all three catalysts, increasing acid to alcohol molar ratio increases conversions of the limiting components and this enhancement in kinetics is more pronounced when the molar ratio is raised from 1 to 2 than when it is raised from 0.5 to 1.

Under the conditions studied, the increase in the catalyst loading is found to increase the percent conversion values for all three catalyst systems. Furthermore, the increase in this value is found to be higher when the catalyst loading is raised from 20 to 40 g/L than when it is raised from 40 to 60 g/L. This work also establishes the effectiveness of gel-type catalysts like Amberlite IR-120 and Dowex 50Wx8 for catalyzing the studied esterification reaction.

The UNIFAC model was found to predict component activity coefficients reasonably well. All six models tried were found to predict the reaction kinetics on the different catalysts under the different conditions studied with mean relative errors $\leq 5.3\%$. Besides proving the adequacy of the models tried, the low error values obtained also prove the success of the UNIFAC model in predicting the activity coefficients of the components present in the system.

The ML model was found to be the best suited for predicting the reaction kinetics of both the gel-type catalysts, Dowex as well as Amberlite, while the PP model was found to be the best to predict reaction kinetics catalyzed by the macroreticular catalyst, Amberlyst. The activation energies for the forward reaction were found to be 57.0, 59.0, and 64.0 kJ/mol for the systems catalyzed by Dowex, Amberlite, and Amberlyst, respectively. The adsorption equilibrium constants of the different components are found to be proportional to their solubility parameters as indicated by the trends in the adsorption equilibrium constants observed for all three catalysts. The ester

molecule is found to contribute insignificantly to the adsorption term for both gel and macroreticular catalyzed systems when their kinetics are represented by the ML and PP models, respectively. The significance of the water adsorption term increases with time and toward the end of the reaction this term dominates over the other component adsorption terms. Throughout the course of the reaction the alcohol adsorption term dominates over the acid adsorption term.

NOMENCLATURE

A_f	Pre-exponential factor for the forward reaction leading to ester formation, mol/g/s
a_i	Activity of the ith component in the liquid phase
a_i'	$(K_i a_i / M_i,)$ mol/g
C_{li}	Limiting reactant concentration in the mixture at a given time in mol/cc
C_W	Weisz Prater parameter
D_e	Effective diffusivity in cm^2/s
D_{li}	Diffusivity of limiting reactant in component i, cm^2/s
D_{lm}	Diffusivity of limiting reactant in the mixture, cm^2/s
ER	Eley Rideal model
E_f	Activation energy for the forward reaction leading to ester formation, J/mol
K	Esterification reaction equilibrium constant
K_i	Adsorption equilibrium constant for species i present in the system
k_f	Forward reaction rate constant for esterification, mol/g/s
LH	Langmuir Hinshelwood model
ML	Modified Langmuir Hinshelwood model
M_{cat}	Mass of the catalyst, g
M_i	Molar mass of component i, g/mol
m^s	Total adsorbed mass, g
m_i^s	Adsorbed mass of component i, g
n	Total number of moles in the system
$n_{samples}$	Number of samples
PH	Pseudohomogeneous model
PP	Pöpken model
PRSV	Peng–Robinson–Stryjek–Vera equation of state
Q	UNIFAC group area parameter
R	UNIFAC group volume parameter
R_g	8.314 J/mol/K (ideal gas law constant)
R_{fit}^2	Correlation coefficient for fitting the K values to Eq. (19)

r_A' (obs)	Observed reaction rate at a given time in mol/g of catalyst/s
R_c	Ratio of catalyst pellet volume to catalyst pellet external surface area in cm
r_{cor}	Correlated reaction rate in mol/s
r_{exp}	Experimental reaction rate obtained by differential method in mol/s
r_i	Reaction rate in mol/s
SG	Staverman–Guggenheim correction term
t	Time in s
T	Temperature in K
x_{exp}	Experimentally determined mole fraction
x_i	Mole fraction of component i
$(x_i)_{eq}$	Mole fraction of component i at equilibrium
x_i^s	Mole fraction of component i in the adsorbate phase
x_{pred}	Predicted mole fraction
γ_i	Activity coefficient of component i
γ_i^{comb}	Combinatorial part of the activity coefficient of component i
γ_i^{res}	Residual part of the activity coefficient of component i
η_i	Viscosity of component i in cp
η_m	Viscosity of the mixture in cp
ξ_v	Void fraction of the catalyst.
ρ_p	Catalyst density in g/cc
ϕ	Objective function
υ_i	Stoichiometric coefficient of component i
α	Exponential term to account for water affinity for the resin
φ_i	Concentration function of component i
Γ_k	Activity coefficient of group k at mixture composition
Γ_k^i	Activity coefficient of group k of pure component i

BIBLIOGRAPHY

1. Simonds, M. R.; Ellis, C. In Handbook of Plastics; Van Nostrand: New York, 1943; pp. 240–271.
2. Kirk, R. E.; Othmer, D. F. In Encyclopedia of Chemical Technology, Japanese reprint edition, 1950; Vol. 5.
3. Carey, F. A. In Advanced Organic Chemistry, 3rd ed.; Plenum Press: New York, 1990.
4. Ogliaruso, M. A.; Wolfe, J. F. In Synthesis of Carboxylic Acids, Esters and Their Derivatives; Wiley: New York, 1991.
5. Xu, Z. P.; Chuang, K. T. Can J Chem Eng 1996, 74, 493–500.
6. Mazzotti, M.; Kruglov, A.; Neri, B.; Gelosa, D.; Morbidelli, M. Chem Eng Sci 1996, 51(10), 1827–1836.
7. Bhatia, S.; Rajamani, K.; Rajkhowa, P.; Gopala Rao, M. Ion Exchange Membr 1973, 1, 127–133.

8. Thorat, T. S.; Yadav, V. M.; Yadav, G. D. Appl Catal A 1992, 90, 73–96.

9. Yadav, G. D.; Kirthivasan, N. J Chem Soc, Chem Commun 1995, 203–204.

10. Yadav, G. D.; Thorat, T. S. Ind Eng Chem Res 1996, 35, 721–732.

11. Yadav, G. D.; Bokade, V. V. Appl Catal A 1996, 147, 299–323.

12. Krishnaiah, D.; Rao, M. B. Indian J Technol 1984, 22, 268–271.

13. Roy, R.; Bhatia, S. J Chem Tech Biotechnol 1987, 37, 1–10.

14. El-Noamany, H. M.; Shaheen, F. A.; El-Kenawy, O. S.; Zaher, F. A. Modelling, Meas Control, C 1993, 43, 25–43.

15. Yadav, G. D.; Mehta, P. H. Ind Eng Chem Res 1994, 33(9), 2198–2208.

16. Bart, H. I.; Kaltenbrunner, W.; Landschutzer, H. Int J Chem Kinet 1996, 28, 649–656.

17. Maki-Arvela, P.; Salmi, T.; Sundell, M.; Ekman, K.; Peltonen, R.; Lehtonen, J. Appl Catal, A 1999, 184, 25–32.

18. Lee, M. J.; Wu, H. T.; Kang, C. H.; Lin, H. M. J Chin Inst Chem Eng 1999, 30(2), 117–122.

19. Lee, M. J.; Wu, H. T.; Lin, H. M. Ind Eng Chem Res 2000, 39, 4094–4099.

20. Pöpken, T.; Gotze, L; Gmehling, J Ind Eng Chem Res 2000, 39, 2601–2611.

21. Kirbaslar, S. I.; Terzioglu, H. Z.; Dramur, U. Chin J Chem Eng 2001, 9(1), 90–96.

22. Lilja, J.; Murzin, D. Y.; Salmi, T.; Aumo, T.; Maki-Arvel, P.; Sundell, M. J Mol Catal A: Chem 2002, 182–183, 555–563.

23. Gangadwala, J.; Mankar, S.; Mahajani, S.; Kienle, A.; Stein, E. Ind Eng Chem Res 2003, 42(10), 2146–2155.

24. El Ewady, Y. A.; El Wakil, A. M.; El Nahas, M. R.; Moussa, M. N. H. J Indian Chem Soc 1984, LXI, 517–519.

25. Awad, M. M. B.; Salem, A. M. A.; Swelam, A. A. J Indian Chem Soc 1997, 74, 467–469.

26. Yadav, G. D.; Thathagar, M. B. React Funct Polym 2002, 52, 99–110.

27. Yadav, G. D.; Kulkarni, H. B. React Funct Polym 2000, 44, 153–165.

28. Leyes, C. E.; Othmer, D. F. Trans Am Inst Chem Eng 1945, 41, 157–196.

29. Petro, M.; Mravec, D.; Ilavsky, J. Chem Zvesti 1983, 37(4), 461–466.

30. Ronnback, R.; Salmi, T.; Vuori, A.; Haario, H.; Lehtonen, J.; Sunsqvist, A.; Tirronen, E. Chem Eng Sci 1997, 52(19), 3369–3381.

31. Kekre, S. Y.; Gopala Rao, M. Ind Chem Eng 1969, 10, 115.

32. Dakshinamurty, P.; Ramarao, M. V. S.; Ramachandramurty, Ch. V. J Chem Technol Biotechnol 1984, 34, 257–261.

33. Chakrabarti, A.; Sharma M. M. React Polym 1993, 20, 1–45.

34. Furniss, B. S.; Hannaford, A. J.; Smith, P. W. G.; Tatchell, A. R. In Vogel's Textbook of Practical Organic Chemistry, 5th ed.; Addison-Welsey/Longman: Harlow, 1989; Chap. 5.

35. McMurry, J. Organic Chemistry; Brooks: Cole, Belmont, 1992; p. 804.

36. Prausnitz, J. M.; Lichtenthaler, R. N.; de Azevedo, E. G. Molecular Thermodynamics of Fluid-Phase Equilibria, 3rd ed.; Prentice-Hall: Englewood Cliff, NJ, 1999.

37. Polyzou, E. N.; Valmos, P. M.; Dimakos, G. M.; Yakoumis, I. V.; Kontogeargis, G. M. Ind Eng Chem Res 1999, 38, 316–323.

38. Steinigeweg, S.; Gmehling, J. Ind Eng Chem Res 2003, 42(15), 3612–3619.

39. Hicks, J. S.; Weisz, P. B. Chem Eng Sci 1962, 17, 265–275.

40. Perkins, L. R.; Geankoplis, C. J. Chem Eng Sci 1969, 24, 1035–1042.

41. Lee, L. S.; Kuo, M. Z. Fluid Phase Equilib 1996, 123, 147–165.

42. Agreda, V. H.; Partin, L. R.; Heise, W. H. Chem Eng Prog 1990, 86(2), 40–46.

43. Toteja, R. S. D.; Jangida, B. L.; Sundaresan, M.; Venkataramani, B. Langmuir 1997, 13(11), 2980–2982.

44. Hansen, K. H.; Coto, B.; Kahlmany, B. SEP 9212, IVC-SEP; Institute of Kemiteknik: Lyngby, Denmark, 1992.

45. Helfferich, F. Ion Exchanger; McGraw-Hill: New York, 1962.

46. Kawase, M.; Suzuki, K.; Inoue, K.; Yoshimoto, K.; Hashimoto, K. Chem Eng Sci 1996, 51(11), 2971–2976.